CHAPTER 5:

IMPURITY PROFILING OF A NOVEL 2-THIO IMIDAZOLE DERIVATIVE ZY12201- AN ANTIDIABETIC AGENT

List of Figures

List of Tables

5.1 Introduction

A large number of antidiabetic drugs have been developed to reverse the insensitivity of muscles, liver and adipose tissue along with improved insulin release pattern in Type 2 diabetic patient till date (1) Structures of oral anti-diabetic drugs are shown in Fig 5.1.

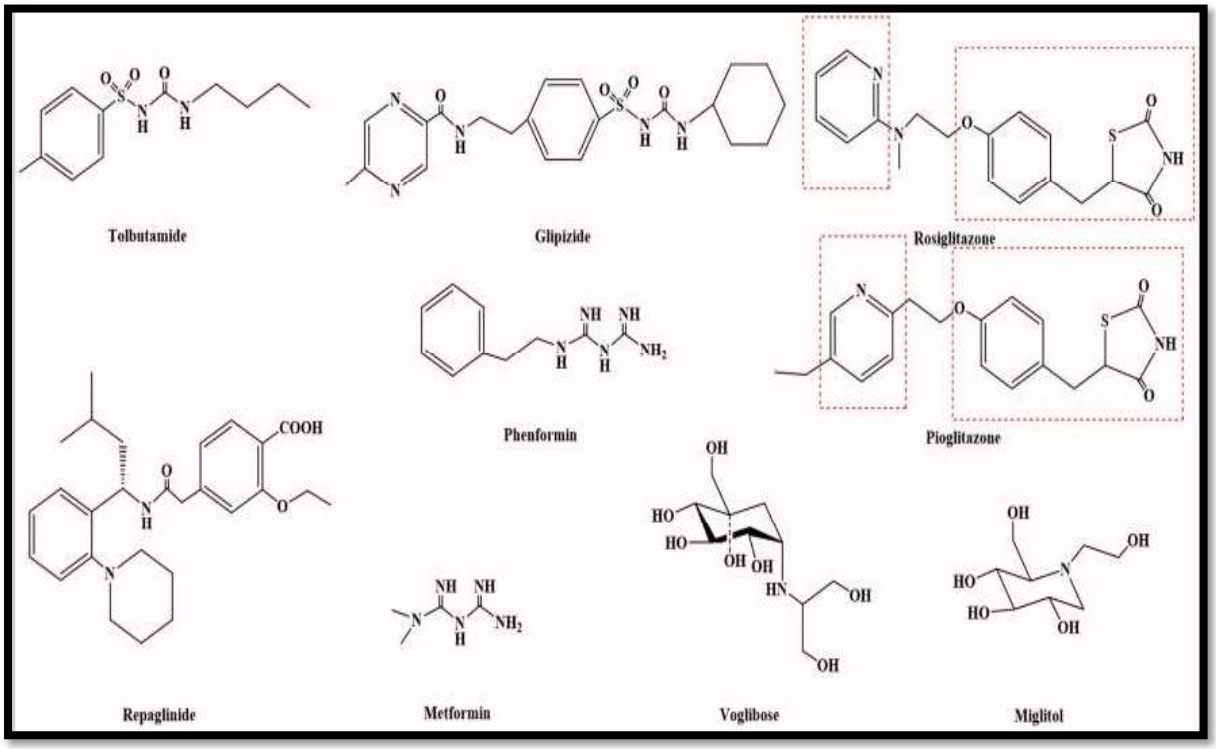

Fig 5.1 The structure of type 2 anti-diabetic drugs

Currently available marketed oral drugs include insulin secretagogues, such as sulphonylureas; peroxisome proliferator-activated receptor-c (PPAR-c) activators i.e. pioglitazone; glucose-lowering molecules i.e. metformin, inhibitors of DPP-IV; GLP-1(glucagon-like peptide-1) analogues and inhibitors of alpha-glucosidase (2,3).However, numbers of patients are not able to control blood glucose level with currently available marketed agents. Therefore, there is an urgent need for exploring new targets with hold mechanism, which is not only dealing with controlling blood glucose or lipid level but taking a challenge of metabolic syndrome as a whole therapy.

TGR5 (Takeda G-protein-coupled receptor 5) is a bile acid G protein receptor popularly known as GPBAR1 (4, 5). TGR5 receptors are activated by bile salts and it is present in gallbladder, brain, liver, spleen and intestine(6). As release of bile acids activate TGR-5 receptor which further induces release of glucagon like peptide from the endocrine cell of intestine by increasing level of cAMP intracellular (7). Moreover, it also increases energy usage through the induction of type 2 iodothyronine deiodinase (D2) (8).Thus, a novel TGR5 agonist

may provide a treatment option for type 2 diabetes with simultaneous management of glucose levels, body weight, and associated complications. A remarkable research has been carried out by Agarwal et al. in the field of the synthesis of novel TGR5 inhibitors (9,10,11). Even researchers have found use of Novel TGR-5 agonist with sitagliptin for the treatment of type - ii diabetes (12). Along with thio-imidazole derivatives Novel derivatives of 2-Mercapto Imidazole and Triazole has been screened for the potential TGR-5 agonist activity (13,14).

Several structurally diverse chemical compounds have been reported as TGR5 modulators by pharmaceutical firms are represented in Fig 5.2 (15,16).

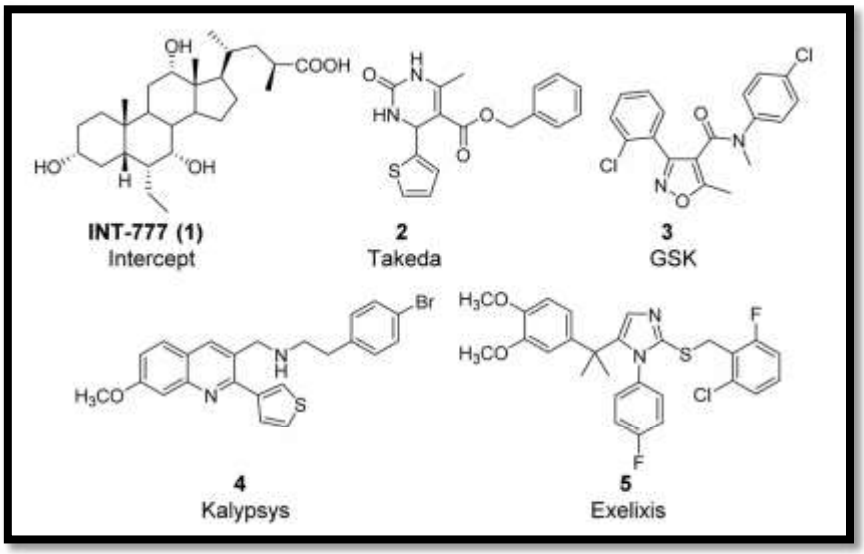

Fig 5.2 Selected bile acid and non-bile acid TGR5 receptor agonist reported in literature

Most of these reported TGR5 agonists, however, possess insufficient potency and/or lack metabolic stability.

5.2 Synthesis and crystallization

ZY12201 is synthesis by reported method (17,18). The synthesis of ZY12201 was accomplished through a seven step process shown in chapter 1. Initially, demethylation of 2-(3,4-dimethoxyphenyl)-acetone using excess of methyl iodide afforded the desired intermediate 2 (3-(3,4-Dimethoxyphenyl)-3-methylbutan-2-one) with 93% yield. Subsequently, X-bromination of compound 2 (3-(3,4-Dimethoxyphenyl)-3-methylbutan-2-one) using tetrabutyl ammonium tribromide afforded a bromo compound 3 (1-Bromo-3-(3,4-dimethoxyphenyl)-3-methylbutan-2-one). In quantitative yield. Compound 3 (1-Bromo-3-(3,4-dimethoxyphenyl)-3-methylbutan-2-one) was transformed to azide 4 (1-Azido-3-(3,4-dimethoxyphenyl)-3-methylbutan-2-one) using sodium azide followed by hydrogenation

provided amine 5 (1-Amino-3-(3,4-dimethoxyphenyl)-3-methylbutan-2-one Hydrochloride) as its corresponding hydrochloride salt. Treatment of amine 5 (1-Amino-3-(3,4-dimethoxyphenyl)-3-methylbutan-2-one Hydrochloride) with 1- fluoro-4- iso thiocynato benzene provided the thiourea. Derivative 6 (1-(3-(3,4-Dimethoxyphenyl)-3-methyl-2-oxobutyl)-3-(4-fluorophenyl)thiourea) treatment of thiourea 6 (1-(3-(3,4-Dimethoxyphenyl)-3-methyl-2-oxobutyl)-3-(4-fluorophenyl)thiourea) in boiling acetic acid led to facile cycliazation, which afforded the 2-thio imidazole derivative 7 (5-(2-(3,4-Dimethoxyphenyl)propan-2-yl)-1-(4-fluorophenyl)-1H-imidazole-2-thiol). Finally, the presence of potassium carbonate afforded ZY12201.

5.3 Single Crystal XRD:

The asymmetric unit of the title compound, $C_{31}H_{31}FN_4O_3S$ is associated with one water molecule. In the crystal, the molecules are apparently linked with their ability to form various CH…π. CH...O. and CH...N contacts, extending conjugation across infinite molecular layers in the solid state. The asymmetric unit mainly forms a number CH...π and CH...O and CH...N intermolecular donor-acceptor contacts with neighboring molecules. The supramolecular assembly arises due to weak noncovalent intermolecular interactions present in crystal packing.

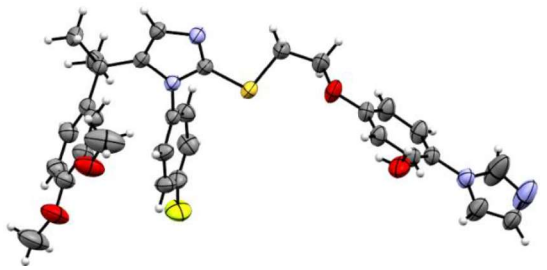

Fig 5.3a 3D view of ZY12201

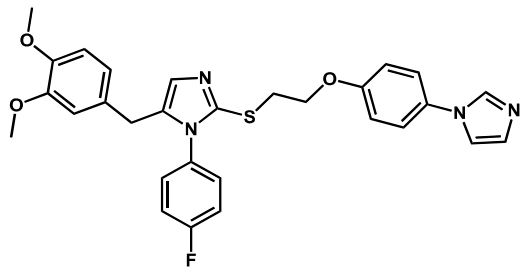

Fig 5.3b Chemical scheme of ZY12201

5.3.1 Structure description

The asymmetric unit contains one molecule of compound and one water solvent molecule as shown in Fig. 5.4.

Intermolecular O—H…N hydrogen bond with water molecules and form macromolecules assembly in solid state as shown in Fig. 5.5 and O—H…N bond distances are 2.875 and 2.991 Å. In the extended structure, the main molecules are linked by N—H…O hydrogen bonds as represented in Table 5.2, to generate [100] stacks as shown in Fig. 5.6 of alternating molecules. The structure is consolidated by C—H…O, C—H… π and C—H…N interactions (which also

involve the solvent molecules as both donors and acceptors), which consolidate the chains into ribbon-like networks Fig. 5.6. All crystallographic parameters are listed in Table 5.3.

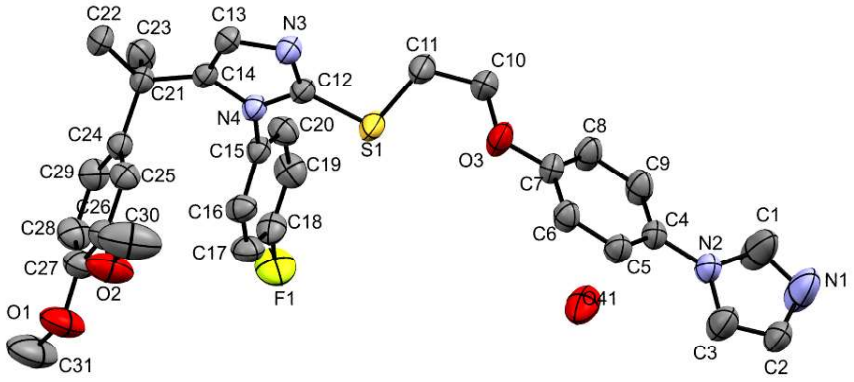

Fig 5.4 Asymmetric unit of title compound showing displacement ellipsoids drawn at the 40% probability level. Hydrogen atoms are omitted for clarity.

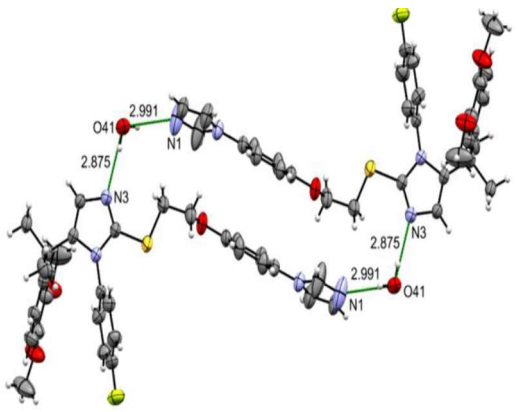

Fig 5.5 Intermolecular O-H…N hydrogen bond with water

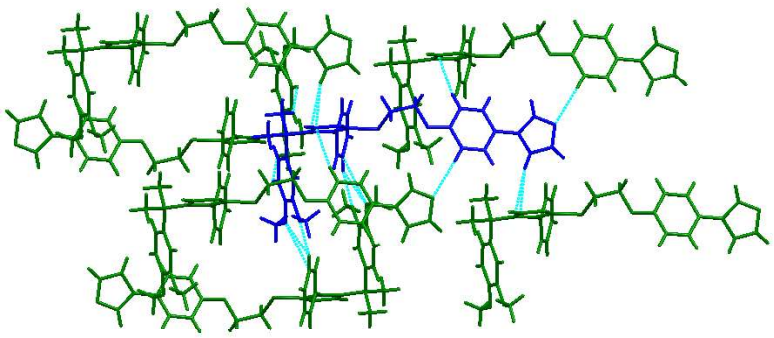

Fig 5.6 Detail of the extended structure showing [100] stacked layer formation of the blue and green molecules due to variation interaction.

Table 5.1 Experimental details for single crystal XRD

Crystal data	
Chemical formula	$C_{31}H_{33}FN_4O_4S$
M_r	576.67
Crystal system, Space group	Triclinic, P-1
a, b, c (Å)	8.8548(6), 10.3539(6) ,16.8284(10)
α, β, γ/°	78.388(5), 80.158(5), 83.078(5)
Temperature/K	293
Volume/$Å^3$	1483.10(16)
Z	2
Radiation type	Mo Kα (λ = 0.71073)
μ (mm^{-1})	0.158
Crystal size (mm)	0.8 ×0.3×0.2
Data collection	
Diffractometer	Agilent Xcalibur, Eos, Gemini
Absorption correction	-
T_{min}, T_{max}	0.945,0.969
No. of measured, independent and observed [I≥2σ (I)] reflections	32734, 7178, 7178
R_{int}	0.0347
Refinement	
$R[F^2>2\sigma(F^2)]$, $wR(F^2)$], S	0.0593, 0.1713, 1.045
No. of reflections	7960
No. of parameters	377
No. of restraints	0
H-atom treatment	H-atom parameters constrained
Δρmax, Δρmin (e A ° $^{-3}$)	0.84, -0.53

Table 5.2 Crystal data and structure refinement	
Empirical formula	$C_{31}H_{33}FN_4O_4S$
Formula weight	576.67
Temperature/K	293.0
Crystal system	Triclinic
Space group	P-1
a/Å	8.8548(6)
b/Å	10.3539(6)
c/Å	16.8284(10)
α/°	78.388(5)
β/°	80.158(5)
γ/°	83.078(5)
Volume/$Å^3$	1483.10(16)
Z	2
ρ_{calc}g/cm^3	1.291
μ/mm^{-1}	0.158
F(000)	608.0
Crystal size/mm^3	0.8 × 0.3 × 0.2
Radiation	MoKα (λ = 0.71073)
2Θ range for data collection/°	6.32 to 58.16
Index ranges	$-11 \leq h \leq 12$, $-14 \leq k \leq 14$, $-21 \leq l \leq 22$
Reflections collected	32734
Independent reflections	7178 [R_{int} = 0.0347, R_{sigma} = 0.0324]
Data/restraints/parameters	7178/0/377
Goodness-of-fit on F^2	1.045
Final R indexes [I>=2σ (I)]	R_1 = 0.0593, wR_2 = 0.1501
Final R indexes [all data]	R_1 = 0.0892, wR_2 = 0.1713
Largest diff. peak/hole / e $Å^{-3}$	0.84/-0.53

Table 5.3 Fractional Atomic Coordinates (×10^4) and Equivalent Isotropic Displacement Parameters (Å^2×10^3) for ZY12201. U_{eq} is defined as 1/3 of of the trace of the orthogonalised U_{IJ} tensor

Atom	*X*	*y*	*z*	U(eq)
S1	5484.4(7)	2189.0(7)	3140.6(4)	59.2(2)
N4	8121.2(18)	1027.2(16)	2417.0(10)	35.3(4)
O3	2756.1(18)	3468.6(16)	4099.3(11)	55.4(4)
N3	8039(2)	881.7(17)	3762.8(10)	41.3(4)
C13	9442(2)	316(2)	3426.5(12)	37.6(4)
F1	5702(2)	2113.3(19)	-481.5(9)	76.6(5)
C4	-1428(2)	5614(2)	3817.1(13)	41.2(5)
C15	7516(2)	1310(2)	1652.5(12)	36.2(4)
C25	11609(3)	2249(2)	1490.0(13)	44.0(5)
C12	7285(2)	1297(2)	3138.6(12)	38.2(4)
C14	9537(2)	393.8(19)	2605.8(12)	34.7(4)
C7	1335(2)	4116(2)	4010.6(13)	42.3(5)
C24	11293(2)	1071(2)	1290.6(13)	39.3(5)
C22	12225(3)	-616(2)	2426.8(15)	52.6(6)
N2	-2860(2)	6393.0(19)	3735.9(12)	48.1(5)
C21	10821(2)	-80(2)	1986.6(13)	38.5(4)
C23	10320(3)	-1223(2)	1670.7(16)	54.2(6)
C20	6476(3)	512(2)	1524.0(14)	47.2(5)
C19	5834(3)	791(3)	811.6(15)	54.2(6)
C5	-148(3)	6212(2)	3879.8(14)	46.2(5)
C16	7906(3)	2408(2)	1069.5(14)	46.8(5)
C6	1232(2)	5468(2)	3965.6(14)	45.6(5)
C26	12039(3)	3314(2)	885.5(14)	50.7(6)
O1	12582(3)	4314(2)	-502.7(11)	81.7(7)
C18	6271(3)	1867(3)	240.9(13)	50.4(6)
C29	11443(3)	993(2)	473.9(14)	49.5(5)

O2	12341(3)	4501.7(18)	1027.4(11)	74.9(6)
C8	60(3)	3510(2)	3965.0(17)	53.7(6)
C17	7276(3)	2690(2)	346.3(14)	53.2(6)
C11	4609(3)	1638(3)	4181.8(14)	54.8(6)
C28	11877(3)	2062(3)	-137.4(15)	58.2(6)
C10	2919(3)	2059(2)	4241.1(17)	57.4(6)
C9	-1321(3)	4271(2)	3858.4(16)	53.3(6)
C2	-4601(3)	8053(3)	3551.5(17)	58.5(6)
C27	12163(3)	3216(3)	53.9(14)	56.2(6)
C3	-3100(3)	7719(3)	3491(2)	69.2(8)
N1	-5352(3)	7015(3)	3891(2)	102.1(11)
C1	-4281(4)	6032(3)	3998(3)	111.9(16)
C31	12834(6)	4207(4)	-1344.9(18)	108.0(14)
C30	12366(6)	4637(4)	1835(2)	112.2(16)
O41	2108(2)	8867(2)	4554.6(11)	74.8(6)

Table5.4 Anisotropic Displacement Parameters ($Å^2 \times 10^3$) for exp_1331. The Anisotropic displacement factor exponent takes the form: $-2\pi^2[h^2a^{*2}U_{11}+2hka^*b^*U_{12}+\ldots]$

Atom	U_{11}	U_{22}	U_{33}	U_{23}	U_{13}	U_{12}
S1	45.1(3)	71.7(4)	45.9(3)	3.3(3)	-2.9(2)	24.4(3)
N4	31.4(9)	38.1(9)	36.0(9)	-6.5(7)	-7.6(6)	1.2(7)
O3	36.7(9)	48.1(9)	80.4(12)	-16.9(8)	-8.6(8)	7.9(7)
N3	39.5(10)	44.1(10)	40.0(9)	-10.2(7)	-8.5(7)	4.9(7)
C13	35.1(11)	38.4(10)	40.2(11)	-7.9(8)	-10.3(8)	1.2(8)
F1	77.5(11)	109.3(13)	46.8(8)	-7.9(8)	-29.3(8)	-6.6(10)
C4	32.3(11)	43.0(11)	46.7(12)	-7.9(9)	-3.3(8)	-0.9(8)
C15	32.5(10)	40.9(11)	35.0(10)	-8.4(8)	-7.7(7)	3.0(8)
C25	48.1(13)	48.7(12)	36.3(11)	-7.7(9)	-8.7(9)	-5.8(10)
C12	36.5(11)	38.3(10)	38.0(10)	-5.9(8)	-6.4(8)	3.2(8)

C14	30.3(10)	31.9(10)	42.3(11)	-6.7(8)	-8.9(8)	-0.1(7)
C7	32.2(11)	45.5(12)	47.8(12)	-11.4(9)	-3.3(8)	3.0(9)
C24	33.2(10)	42.6(11)	41.1(11)	-7.7(9)	-5.5(8)	0.5(8)
C22	36.8(12)	56.7(14)	56.5(14)	-2.0(11)	-4.7(10)	9.0(10)
N2	33.0(10)	46.4(11)	61.4(12)	-3.0(9)	-6.2(8)	-2.6(8)
C21	32.7(10)	39.0(11)	42.6(11)	-8.9(8)	-4.3(8)	1.9(8)
C23	58.0(15)	44.4(13)	59.0(15)	-19.0(11)	5.5(11)	-3.7(11)
C20	47.2(13)	50.2(13)	44.7(12)	-6.1(10)	-7.4(9)	-10.8(10)
C19	50.6(14)	67.9(16)	50.7(13)	-16.0(12)	-13.6(10)	-15.1(12)
C5	38.9(12)	37.5(11)	60.5(14)	-7.0(10)	-5.3(10)	-3.6(9)
C16	45.5(13)	43.3(12)	52.1(13)	-1.2(10)	-16.3(10)	-6.0(9)
C6	33.9(11)	44.6(12)	59.2(14)	-11.8(10)	-5.6(9)	-5.6(9)
C26	60.7(15)	46.1(13)	45.4(12)	-6.4(10)	-7.8(10)	-9.1(11)
O1	127(2)	64.3(12)	45.7(10)	3.1(9)	2.5(11)	-19.2(12)
C18	46.5(13)	68.8(15)	36.8(11)	-11.5(10)	-14.1(9)	5.6(11)
C29	56.5(14)	49.8(13)	44.6(12)	-16.7(10)	-6.3(10)	-3.2(11)
O2	123.1(18)	53.7(11)	52.2(11)	-3.4(8)	-16.2(11)	-32.0(11)
C8	41.9(13)	39.9(12)	80.2(17)	-18.8(11)	-5.0(11)	-0.9(10)
C17	55.2(14)	54.6(14)	45.2(13)	6.8(10)	-14.2(10)	-4.1(11)
C11	49.4(14)	61.1(15)	44.7(13)	-4.0(11)	-2.3(10)	15.5(11)
C28	73.1(18)	62.9(16)	37.5(12)	-11.8(11)	-4.7(11)	-2.8(13)
C10	46.0(14)	50.0(14)	65.3(15)	-2.2(11)	3.9(11)	7.6(11)
C9	35.2(12)	50.9(13)	77.0(17)	-18.0(12)	-7.4(11)	-8.0(10)
C2	40.6(13)	52.7(14)	76.3(17)	-2.8(12)	-11.3(11)	6.5(11)
C27	68.3(17)	52.8(14)	42.4(13)	-1.6(10)	-3.0(11)	-5.0(12)
C3	46.7(15)	52.3(15)	105(2)	-6.8(14)	-15.6(14)	1.2(12)
N1	45.4(15)	70.2(18)	185(3)	-12.4(19)	-21.7(17)	3.2(13)
C1	45.6(18)	58.3(19)	218(5)	10(2)	-20(2)	-9.6(14)
C31	174(4)	86(2)	46.7(17)	5.7(15)	9(2)	-10(3)
C30	204(5)	75(2)	75(2)	-7.9(17)	-50(3)	-53(3)

O41	72.4(14)	101.2(16)	47.0(10)	-15.2(10)	-19.9(9)	25.3(11)

Table 5.5 Bond Lengths

Atom	Atom	Length/Å	Atom	Atom	Length/Å
S1	C12	1.744(2)	C24	C29	1.376(3)
S1	C11	1.799(2)	C22	C21	1.544(3)
N4	C15	1.440(2)	N2	C3	1.354(3)
N4	C12	1.371(3)	N2	C1	1.332(4)
N4	C14	1.399(2)	C21	C23	1.530(3)
O3	C7	1.370(2)	C20	C19	1.378(3)
O3	C10	1.424(3)	C19	C18	1.363(3)
N3	C13	1.387(3)	C5	C6	1.377(3)
N3	C12	1.312(3)	C16	C17	1.389(3)
C13	C14	1.356(3)	C26	O2	1.364(3)
F1	C18	1.360(2)	C26	C27	1.408(3)
C4	N2	1.430(3)	O1	C27	1.364(3)
C4	C5	1.384(3)	O1	C31	1.421(4)
C4	C9	1.370(3)	C18	C17	1.359(3)
C15	C20	1.379(3)	C29	C28	1.392(3)
C15	C16	1.381(3)	O2	C30	1.398(4)
C25	C24	1.398(3)	C8	C9	1.391(3)
C25	C26	1.383(3)	C11	C10	1.499(3)
C14	C21	1.512(3)	C28	C27	1.361(4)
C7	C6	1.379(3)	C2	C3	1.324(4)
C7	C8	1.376(3)	C2	N1	1.311(4)
C24	C21	1.536(3)	N1	C1	1.311(4)

Table 5.6 Bond Angles for ZY12201							
Atom	**Atom**	**Atom**	**Angle/°**	**Atom**	**Atom**	**Atom**	**Angle/°**
C12	S1	C11	100.76(10)	C14	C21	C23	109.45(17)
C12	N4	C15	123.07(16)	C24	C21	C22	108.35(17)
C12	N4	C14	106.57(16)	C23	C21	C24	112.39(18)
C14	N4	C15	130.26(16)	C23	C21	C22	107.83(18)
C7	O3	C10	118.89(18)	C19	C20	C15	120.5(2)
C12	N3	C13	104.59(17)	C18	C19	C20	118.0(2)
C14	C13	N3	111.76(17)	C6	C5	C4	120.3(2)
C5	C4	N2	119.85(19)	C15	C16	C17	119.8(2)
C9	C4	N2	120.58(19)	C5	C6	C7	120.1(2)
C9	C4	C5	119.5(2)	C25	C26	C27	119.6(2)
C20	C15	N4	119.40(18)	O2	C26	C25	124.8(2)
C20	C15	C16	119.99(19)	O2	C26	C27	115.5(2)
C16	C15	N4	120.52(19)	C27	O1	C31	117.1(2)
C26	C25	C24	121.2(2)	F1	C18	C19	118.4(2)
N4	C12	S1	120.15(15)	C17	C18	F1	118.1(2)
N3	C12	S1	127.46(16)	C17	C18	C19	123.5(2)
N3	C12	N4	112.27(18)	C24	C29	C28	121.0(2)
N4	C14	C21	124.48(17)	C26	O2	C30	118.7(2)
C13	C14	N4	104.80(17)	C7	C8	C9	119.6(2)
C13	C14	C21	130.71(18)	C18	C17	C16	118.1(2)
O3	C7	C6	115.42(19)	C10	C11	S1	107.89(16)
O3	C7	C8	124.5(2)	C27	C28	C29	121.1(2)
C8	C7	C6	120.1(2)	O3	C10	C11	107.0(2)
C25	C24	C21	118.97(18)	C4	C9	C8	120.5(2)
C29	C24	C25	118.1(2)	N1	C2	C3	109.9(2)
C29	C24	C21	122.9(2)	O1	C27	C26	115.9(2)

C3	N2	C4	128.0(2)	C28	C27	C26	119.0(2)
C1	N2	C4	128.4(2)	C28	C27	O1	125.1(2)
C1	N2	C3	102.8(2)	C2	C3	N2	108.7(2)
C14	C21	C24	110.47(16)	C2	N1	C1	104.9(3)
C14	C21	C22	108.22(17)	N1	C1	N2	113.4(3)

Table 5.7 Hydrogen Atom Coordinates (Å×10^4) and Isotropic Displacement Parameters (Å^2×10^3) for exp_1331

Atom	*X*	*Y*	*z*	U(eq)
H13	10222	-71	3727	45
H25	11528	2317	2039	53
H22A	12559	83	2634	79
H22B	13046	-942	2046	79
H22C	11942	-1322	2874	79
H23A	10018	-1911	2126	81
H23B	11161	-1568	1309	81
H23C	9466	-909	1379	81
H20	6205	-221	1921	57
H19	5124	263	723	65
H5	-220	7120	3864	55
H16	8590	2958	1161	56
H6	2096	5877	3993	55
H29	11251	215	328	59
H8	122	2596	4005	64
H17	7533	3422	-55	64
H11A	4776	682	4329	66
H11B	5060	2028	4554	66
H28	11974	1985	-685	70
H10A	2484	1739	3834	69

H10B	2391	1705	4781	69
H9	-2178	3866	3815	64
H2	-5055	8898	3379	70
H3	-2337	8300	3309	83
H1	-4492	5168	4234	134
H31A	13253	4992	-1670	162
H31B	11876	4107	-1510	162
H31C	13545	3450	-1424	162
H30A	12633	5507	1838	168
H30B	13114	3987	2069	168
H30C	11368	4510	2152	168
H41A	2154	8938	5044	112
H41B	2715	8213	4429	112

5.4 Crystal structure determination of ZY12201

Crystal Data for $C_{31}H_{33}FN_4O_4S$ (M =576.67 g/mol): triclinic, space group P-1 (no. 2), a = 8.8548(6) Å, b = 10.3539(6) Å, c = 16.8284(10) Å, α = 78.388(5)°, β = 80.158(5)°, γ = 83.078(5)°, V = 1483.10(16) Å^3, Z = 2, T = 293.0 K, μ(MoKα) = 0.158 mm^{-1}, $Dcalc$ = 1.291 g/cm^3, 32734 reflections measured (6.32° ≤ 2Θ ≤ 58.16°), 7178 unique (R_{int} = 0.0347, R_{sigma} = 0.0324) which were used in all calculations. The final R_1 was 0.0593 (>2sigma(I)) and wR_2 was 0.1713 (all data).

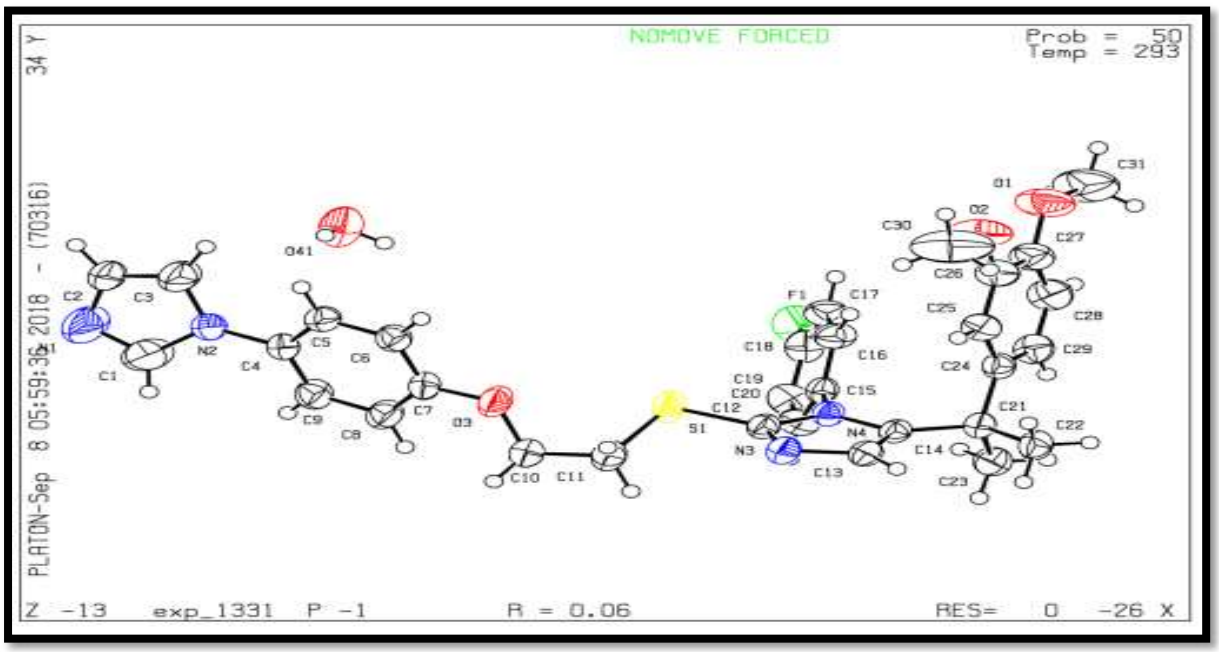

Fig 5.7 ORTEP image of ZY12201

5.5 Materials and Equipments:

5.5.1 Materials and Reagents

ZY12201 standards and samples were synthesized in Zydus Research Center, Cadila Healthcare Ltd. (Ahmedabad, India). HPLC grade acetonitrile and ammonia solution and analytical grade ammonium acetate, hydrogen peroxide solution (30%) were purchased from Merck SpecialtiesPvt. Ltd. (Mumbai, India). High purity HPLC grade water was prepared by using Millipore Milli-Q plus water purification system, Bradford, PA, USA

5.5.2 Equipments:

Equipment/Instrument	Manufacture
Waters HPLC-PDA system	Milford, MA, USA
Prominence Electrospray LC–MS system	Shimadzu, Japan
Analytical balance/ Micro balance	Mettler Toledo, USA
Sonicator	PCI Analytics, India

Table 5.8 Equipments and instruments used

Detector wavelength was 228 nm and data processed using Empower 3 software; Version builds 3471. The column used for chromatography was YMC Triat C18 150 mm, 4.6 mm and 3 µm particle size.

5.5.3 Preparation of Solutions

Preparation of solutions

Preparation of standard stock solutions for validation

ZY12201 stock solutions were prepared with a concentration of 1000 µg/ml in diluent.

Preparation of sample solution

ZY12201 test solutions of concentration 1000 µg/ml in diluents, sonicated for 5 mins to dissolve and were further analyzed by HPLC.

5.6 Chromatographic method development conditions:

Method development trials	Parameter	Outcome
Trial-1	**Column**: Hypersil BDS C18 (150 mm × 4.6 mm, 5 µm) **Mobile phase** M.P-A : 0.1% TFA in water MP-B: Acetonitrile	In this trial, negative baseline was observed and poor chromatography observed
Trial-2	**Column:** Inertsil C8-3 (250 mm × 4.6 mm, 5 µm) **Mobile phase** M.P-A : 0.1% TFA in water MP-B: Acetonitrile	Peak shape of ZY12201 was poor with tailing and low theoretical plates.
Trial-3	**Column:** Sunniest C18 (250 mm × 4.6 mm, 5 µm) **Mobile phase** M.P-A : Ammonium acetate Buffer with pH 4.5 MP-B: Acetonitrile	Peak shape of ZY12201 was poor with tailing and low theoretical plates.
Trial-3	**Column:**Sunfire C18 (250 mm × 4.6 mm, 5 µm) **Mobile phase** M.P-A : Triethyl amine buffer solution pH 6.5 ±0.05 MP-B: methanol, acetonitrile in 50:50 %, v/v	Peak shape of ZY12201 was poor with tailing and low theoretical plates.

Trial-4	**Column:**YMC Triat C18 (150 mm × 4.6 mm, 3 µm) **Mobile phase** M.P-A : 10mM ammonium acetate (pH 8.5) with ammonia solution M.P-B : Acetonitrile	Peak shape and chromatography was good only negative baseline was observed so needs to be optimized.
Trial-5	**Column:**YMC Triat C18 (150 mm × 4.6 mm, 3 µm) **Mobile phase** M.P-A : 10mM ammonium acetate (pH 8.5) with ammonia solution M.P-B : 0.1% Ammonia in Acetonitrile	Peak shape and chromatography was good

Table 5.9 Trials for the chromatographic development

Parameter	**Conditions**		
HPLC Column	YMC Triat C18 (150mm X 4.6mm i.d., 3µm particle size)		
Mobile Phase	A: 10mM ammonium acetate (pH 8.5) with ammonia solution		
	B: 0.1% Ammonia in Acetonitrile		
Injection Volume	15 µL		
Flow Rate	1.2 mL/min		
Column Oven Temp.	35º C		
UV Wavelength	UV Detector – 228 nm		
Run Time (min)	27.2 min		
Diluent	Acetonotrile:Water-95:5%v/v		
Gradient Programming	Time	%A	%B
	0.01	98	2
	3	98	2
	10	60	40
	20	60	40
	32	20	80
	40	20	80
	45	98	2

Table 5.10 LC method parameters

5.7 Force degradation study

Forced degradation studies have proved useful in analyzing stability of pharmaceutical products in different conditions. Stability studies can be useful in formulation selection, packaging selection and storage conditions for the products. Nowadays, stability data and force degradation studies are the major point of discussion among regulatory bodies (19).

ICH mandates to provide force degradation studies of new drug products along with information about potential degradants from force degradation. From the force degradation studies degradation pathways of drug products can be clarified and we can prevent it from degradation. Probable polymorphic conversion of drug product and cross reaction between drug-excipients during storage can be assessed by forced degradation studies (20). As per ICH guidelines force degradation studies should be performed under different conditions of pH, light, oxidation, dry heat, acidic, basic, hydrolysis etc. (21).The FDA and ICH guidance mandate the requirement of forced degradation to recognize how the quality of a drug substance and drug product varies with time and different environmental factors (22, 23).

5.7.1 Outcomes of forced degradation studies(24, 25)

- ✓ Intrepidity of likely degradants
- ✓ Intrepidity of degradation pathways
- ✓ Intrepidity of stability (intrinsic) of the drug molecule
- ✓ Intrepidity of stability (validated) indicating analytical methods

5.7.2 Objective for forced degradation

First objective was to develop degradation pathways of drug products and to recognize the chemical properties of drug substance(26). From force degradation study one can elucidate the structure of degradation products along with resolution of stability-related problems.From these type of studies we can produce more stable formulations of drugs and it also helps in determination of expiry date of drugs. To generate a degradation profile similar to that of what would be observed in a formal stability study under ICH conditions(27, 28).

5.8 Various degradation conditions

The structural variety of drugs makes it very difficult for development of common force degradation set of protocol. The stress conditions applied should be related to the product's nature of decomposition (29). The selected approach must include products property along with details on its degradation under normal process of manufacturing, storage conditions and used conditions. Below Figure 5.8 shows the approach for forced degradation.

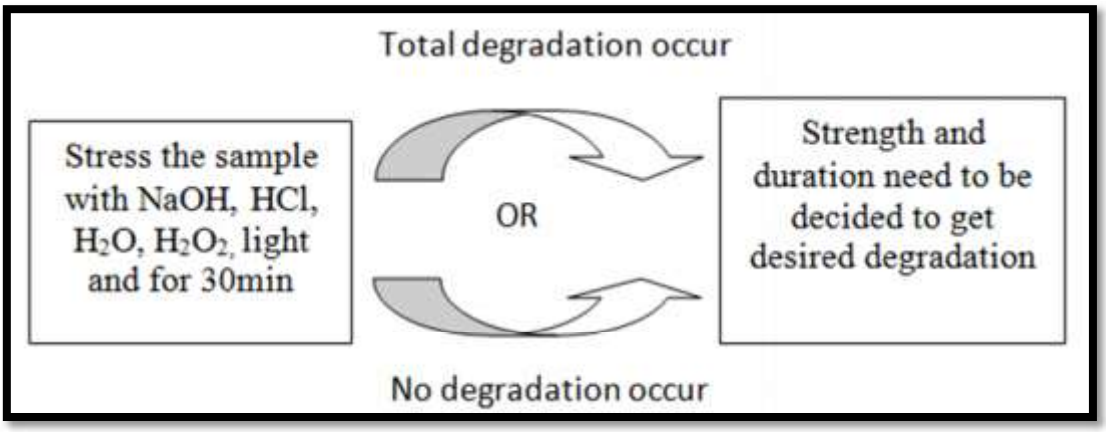

Fig 5.8 Approach for Forced Degradation.

Forced degradation factors necessarily include acid and base hydrolysis, thermal degradation, photolysis, and oxidation and may include freeze-thaw cycles and shear(30). General conditions used for forced degradation were illustrated in Table 5.11.

Degradation Type	Experimental Conditions	Storage Conditions	Sampling Time (days)
Hydrolysis	Control API (no acid or base	40˚C, 60˚C	1,3,5
	0.1M HCl	40˚C, 60˚C	1,3,5
	0.1 M NaOH	40˚C, 60˚C	1,3,5
	Acid control (no API)	40˚C, 60˚C	1,3,5
	Base control (no API)	40˚C, 60˚C	1,3,5
	pH: 2,4,6,8	40˚C, 60˚C	1,3,5
Oxidation	3% H2 O2	25˚C, 60˚C	1,3,5
	Peroxide control	25˚C, 60˚C	1,3,5
	Azobisisobutyronitrile (AIBN)	25˚C, 60˚C	1,3,5
	AIBN control	25˚C, 60˚C	1,3,5

Photolytic	Light 1 × ICH	NA	1,3,5
	Light 2 × ICH	NA	1,3,5
	Light 3 × ICH	NA	1,3,5
Thermal	Heat chamber	60˚	1,3,5
	Heat chamber	C 60˚C /75% RH	1,3,5
	Heat chamber	60˚C	1,3,5
	Heat chamber	60˚C /75% RH	1,3,5

Table 5.11 General conditions used for forced degradation

5.8.1 Control sample

Control sample prepared and Injected to HPLC (1mg/mL). HPLC purity chromatogram for control sample is shown below in Fig 5.9.

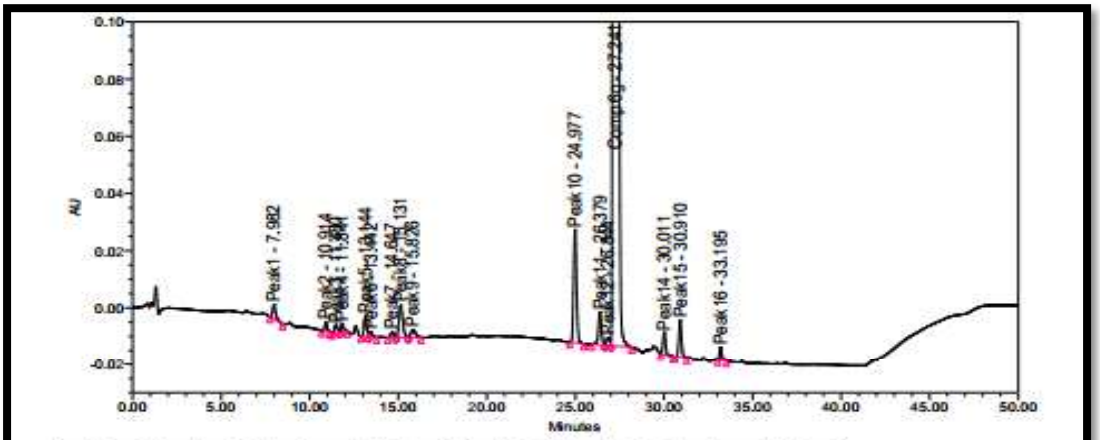

	Peak Name	RT	Area	% Area
1	Peak1	7.982	62345	0.15
2	Peak2	10.914	30197	0.07
3	Peak3	11.480	31595	0.08
4	Peak4	11.841	28468	0.07
5	Peak5	13.144	74555	0.18
6	Peak6	13.442	23405	0.06
7	Peak7	14.647	19275	0.05
8	Peak8	15.131	164861	0.40
9	Peak9	15.826	47547	0.12
10	Peak10	24.977	460236	1.13

	Peak Name	RT	Area	% Area
11	Peak11	26.379	136821	0.33
12	Peak12	26.844	33291	0.08
13	Comp 6g	27.241	39518165	96.62
14	Peak14	30.011	81132	0.20
15	Peak15	30.910	140015	0.34
16	Peak16	33.195	47697	0.12

Fig 5.9 Control sample HPLC purity chromatogram

5.8.2 Hydrolysis:

Hydrolysis is a common degradation reaction which can occur over a wide pH range. Hydrolysis of a drug product or substance can occur when the active compound interacts with acid and base. It produces primary degradants in the measurable range. Choice of concentrations and choice of acid bases depend on the stability of active pharmaceutical ingredient. For acid treated hydrolysis generally hydrochloric acid or sulphuric acids in concentrations of 0.1 to 1 M can be considered suitable whereas for base hydrolysis sodium hydroxide or potassium hydroxides in concentration range of0.1 to 1M are generally taken (29, 31).Sometimes organic solvents like methanol, acetonitrile, dichloromethane etc.can be used for poorly soluble compounds in water. Forced degradation was started at room temperature and further temperature increased if no degradation was observed.

Sample was treated with 1 ml of 5.0M hydrochloric acid solution and heated at 60°C for 120 minutes. HPLC Chromatogram for Acid Treated sample is shown in Fig 5.10 and sample for the alkali treated is shown in Fig. 5.11. For alkali degradation, sample was treated with 1 ml of 5.0M Sodium hydroxide solution and heated at 60°C for 120 minutes.

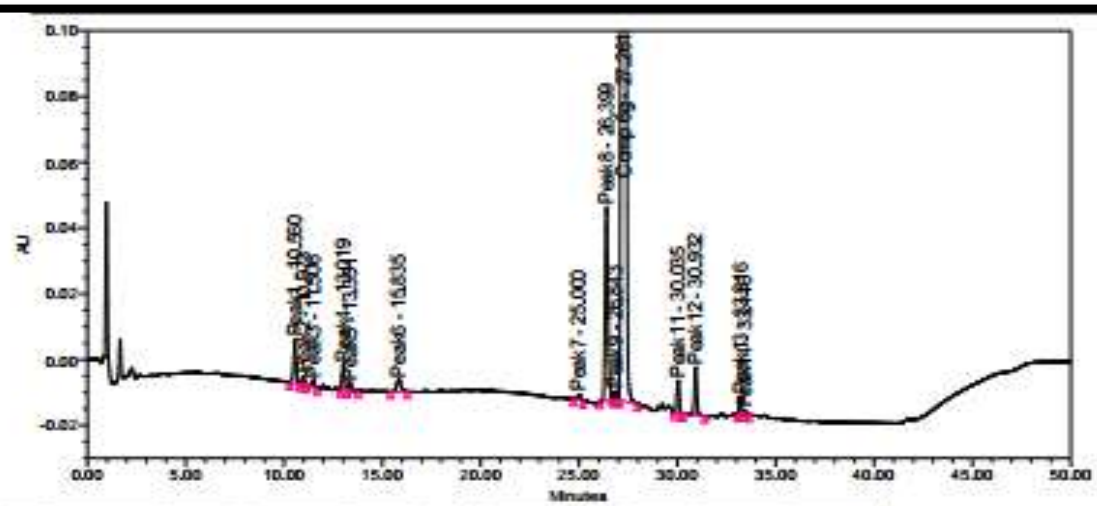

	Peak Name	RT	Area	% Area
1	Peak1	10.560	117287	0.37
2	Peak2	10.973	21188	0.07
3	Peak3	11.506	22414	0.07
4	Peak4	13.019	66794	0.21
5	Peak5	13.351	22363	0.07
6	Peak6	15.835	54024	0.17
7	Peak7	25.000	17011	0.05
8	Peak8	26.399	613550	1.95
9	Peak9	26.843	28196	0.09
10	Comp 6g	27.261	30292953	96.07

	Peak Name	RT	Area	% Area
11	Peak11	30.035	90459	0.29
12	Peak12	30.932	133626	0.42
13	Peak13	33.216	43084	0.14
14	Peak14	33.416	8908	0.03

Fig 5.10 Purity chromatogram of Acid treated sample

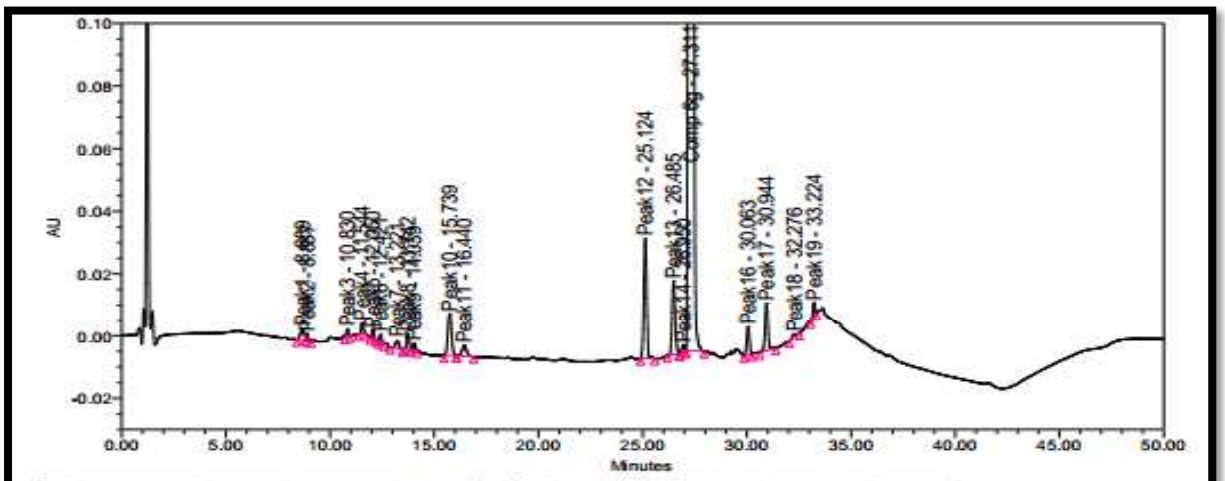

	Peak Name	RT	Area	% Area
1	Peak1	8.689	46530	0.15
2	Peak2	8.887	17224	0.05
3	Peak3	10.830	15407	0.05
4	Peak4	11.544	28176	0.09
5	Peak5	12.050	18398	0.06
6	Peak6	12.421	16553	0.05
7	Peak7	13.221	27529	0.09
8	Peak8	13.742	40992	0.13
9	Peak9	14.039	20106	0.06
10	Peak10	15.739	166976	0.53

	Peak Name	RT	Area	% Area
11	Peak11	16.440	50604	0.16
12	Peak12	25.124	380043	1.21
13	Peak13	26.485	240807	0.77
14	Peak14	26.950	20221	0.06
15	Comp 6g	27.311	30089561	95.65
16	Peak16	30.063	83150	0.26
17	Peak17	30.944	150397	0.48
18	Peak18	32.276	10185	0.03
19	Peak19	33.224	36455	0.12

Fig 5.11 Purity chromatogram of Alkali treated sample

5.8.3 Oxidation:

Hydrogen peroxide is widely used for the oxidative stress degradation. Apart from hydrogen peroxide ions of different metals, oxygen purging and radical initiators like Azobisisobutyronitrile (AIBN) can be used. Electron transfer serves as basic mechanism for the oxidative forced degradation of drug substance (32). HPLC Chromatogram for oxidation treated sample is shown in Fig 5.12. Sample was treated with 1 ml of 3% hydrogen peroxide solution and kept at room temperature for 4h.

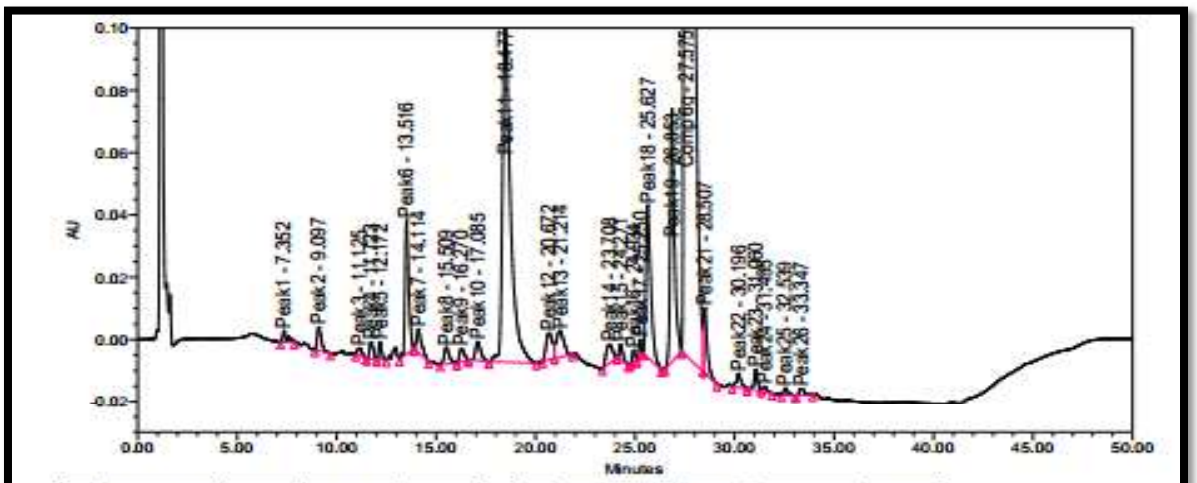

	Peak Name	RT	Area	% Area
1	Peak1	7.352	53659	0.15
2	Peak2	9.097	112682	0.31
3	Peak3	11.125	38292	0.11
4	Peak4	11.723	70451	0.19
5	Peak5	12.172	59753	0.16
6	Peak6	13.516	550438	1.52
7	Peak7	14.114	131948	0.36
8	Peak8	15.509	95036	0.26
9	Peak9	16.270	68518	0.19
10	Peak10	17.085	114631	0.32

	Peak Name	RT	Area	% Area
11	Peak11	18.477	3086675	8.50
12	Peak12	20.672	189782	0.52
13	Peak13	21.214	223653	0.62
14	Peak14	23.708	135305	0.37
15	Peak15	24.271	60708	0.17
16	Peak16	24.934	37361	0.10
17	Peak17	25.250	51415	0.14
18	Peak18	25.627	841549	2.32
19	Peak19	26.853	1203093	3.31
20	Comp 6g	27.575	28690747	78.98

Fig 5.12 Purity chromatogram of Oxidation treated sample

5.8.4 Photolytic condition:

The effect on drug substance upon exposure of light can be tested by photolytic degradation method. Photo stability studies are performed to produce primary degradants of drug substance by exposure to UV or fluorescent conditions. According to ICH guidelines some of recommended conditions protocols for photo stability studies are described here (33). Samples are exposed to a minimum light of 1.2million lx h and 200 W h/ m^2 light. 300-800 nm wavelengths are commonly used to cause the photolytic degradation(34). Free radical mechanism was proposed for photolytic degradation. Carbonyls, nitro aromatic, N-oxide, alkenes, aryl chlorides, weak C–H and O–H bonds, sulfides and polyenes are example of photosensitive groups present in pharmaceuticals(35,36). Sample was exposed for UV degradation under a UV lamp at 254 nm for 24 h. HPLC Chromatogram for UV treated sample is shown in Fig 5.13.

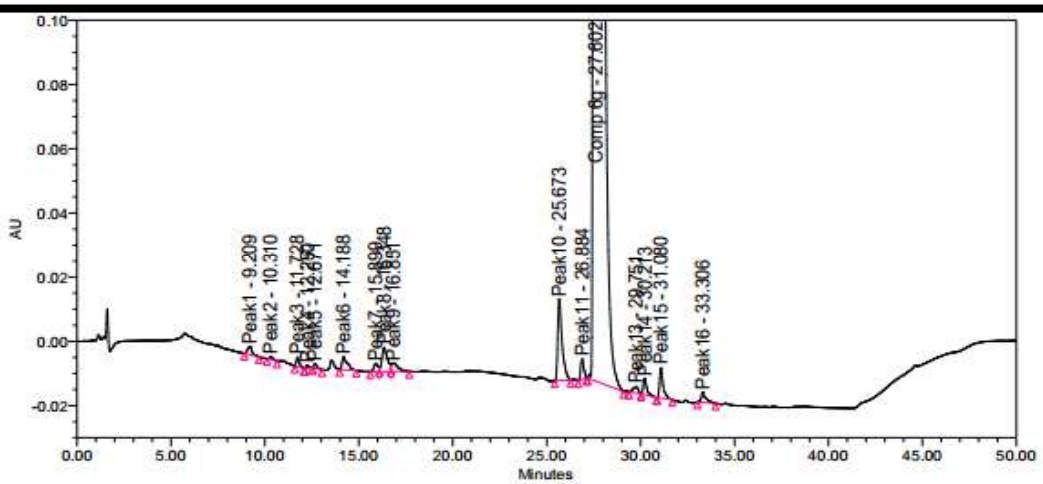

	Peak Name	RT	Area	% Area
1	Peak1	9.209	41749	0.10
2	Peak2	10.310	11590	0.03
3	Peak3	11.728	32544	0.08
4	Peak4	12.250	9235	0.02
5	Peak5	12.671	13125	0.03
6	Peak6	14.188	77288	0.18
7	Peak7	15.899	37720	0.09
8	Peak8	16.348	153794	0.36
9	Peak9	16.851	62999	0.15
10	Peak10	25.673	411739	0.96

	Peak Name	RT	Area	% Area
11	Peak11	26.884	75202	0.18
12	Comp 6g	27.602	41651845	97.18
13	Peak13	29.751	37873	0.09
14	Peak14	30.213	66037	0.15
15	Peak15	31.080	125030	0.29
16	Peak16	33.306	53728	0.13

Fig 5.13 Purity chromatogram of UV treated sample

5.8.5 Thermal conditions:

Thermal degradation can be carried out by dry heat or wet heat. Solid drugs should be exposed to dry and wet heat. Liquid drugs should be exposed to dry heat. For a short duration studies should be conducted with higher temperatures. Sample was kept for thermal degradation at 105°C for 24 h. HPLC Chromatogram for thermal treated sample is shown in Fig 5.14.

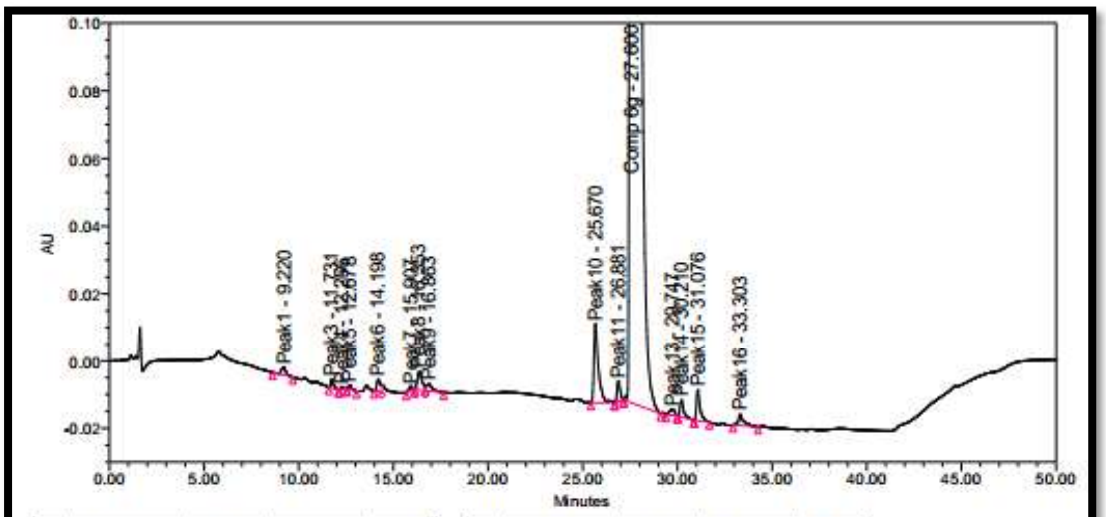

	Peak Name	RT	Area	% Area
1	Peak1	9.220	39979	0.10
2	Peak3	11.731	28271	0.07
3	Peak4	12.256	7213	0.02
4	Peak5	12.678	13208	0.03
5	Peak6	14.198	45158	0.11
6	Peak7	15.907	17231	0.04
7	Peak8	16.353	92434	0.23
8	Peak9	16.863	44445	0.11
9	Peak10	25.670	389471	0.96
10	Peak11	26.881	69205	0.17

	Peak Name	RT	Area	% Area
11	Comp 6g	27.600	39483876	97.46
12	Peak13	29.747	32998	0.08
13	Peak14	30.210	65416	0.16
14	Peak15	31.076	119294	0.29
15	Peak16	33.303	63962	0.16

Fig 5.14 Purity chromatogram of thermally treated sample

5.8.6 Peak purity:

Peak purity is a comparison of the reference standard to the API in the sample stressed by forced degradation (thus specificity). In essence you are showing that no impurity (related substance) is eluting underneath the main API peak in HPLC. Peak threshold is used as a parameter for determining peak purity in HPLC. For the acceptance of the peak purity, angle should be less than a purity threshold.

Degradation condition	Acid treated	Alkali treated	Oxidation Treated	Photolytic treated	Thermal Treated
Purity angle	3.467	3.557	0.702	1.855	1.512
Purity threshold	5.716	5.390	1.344	3.001	2.450

Table 5.12 Peak purity table

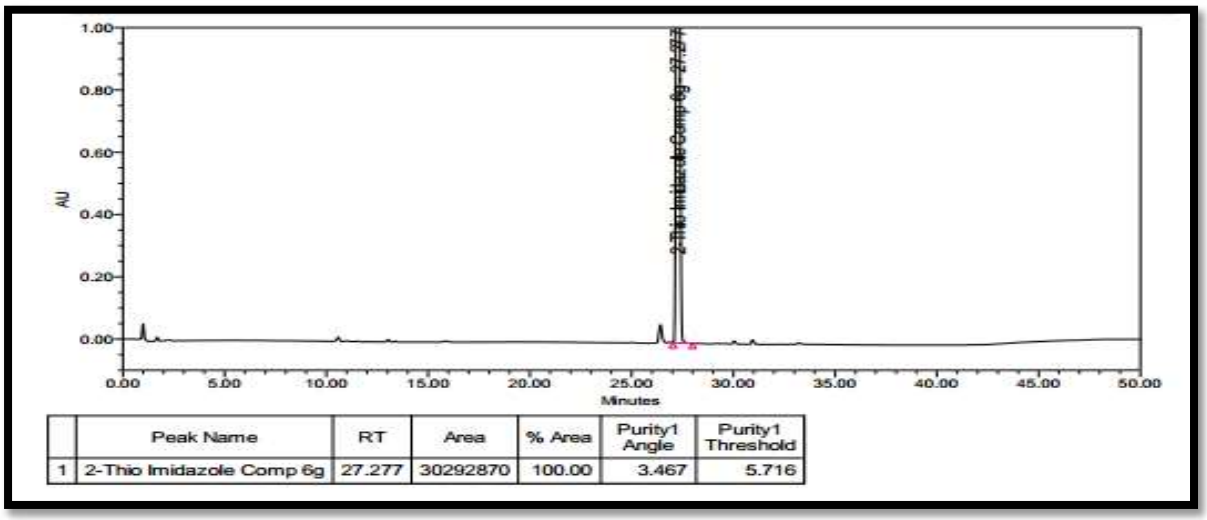

	Peak Name	RT	Area	% Area	Purity1 Angle	Purity1 Threshold
1	2-Thio Imidazole Comp 6g	27.277	30292870	100.00	3.467	5.716

Fig 5.15 Peak purity of acid treated sample

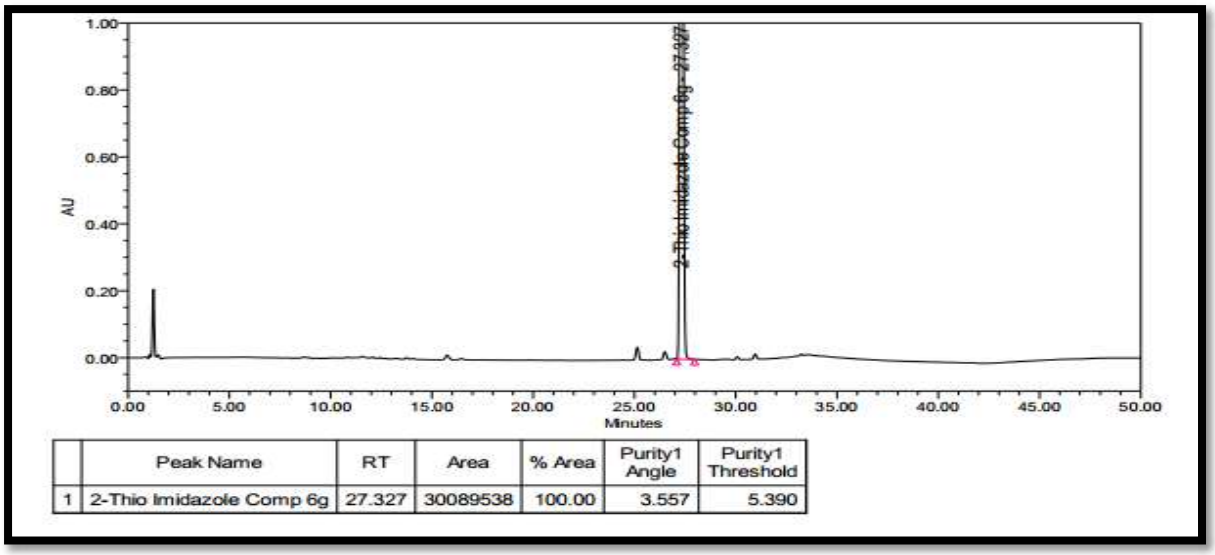

	Peak Name	RT	Area	% Area	Purity1 Angle	Purity1 Threshold
1	2-Thio Imidazole Comp 6g	27.327	30089538	100.00	3.557	5.390

Fig 5.16 Peak purity of alkali treated sample

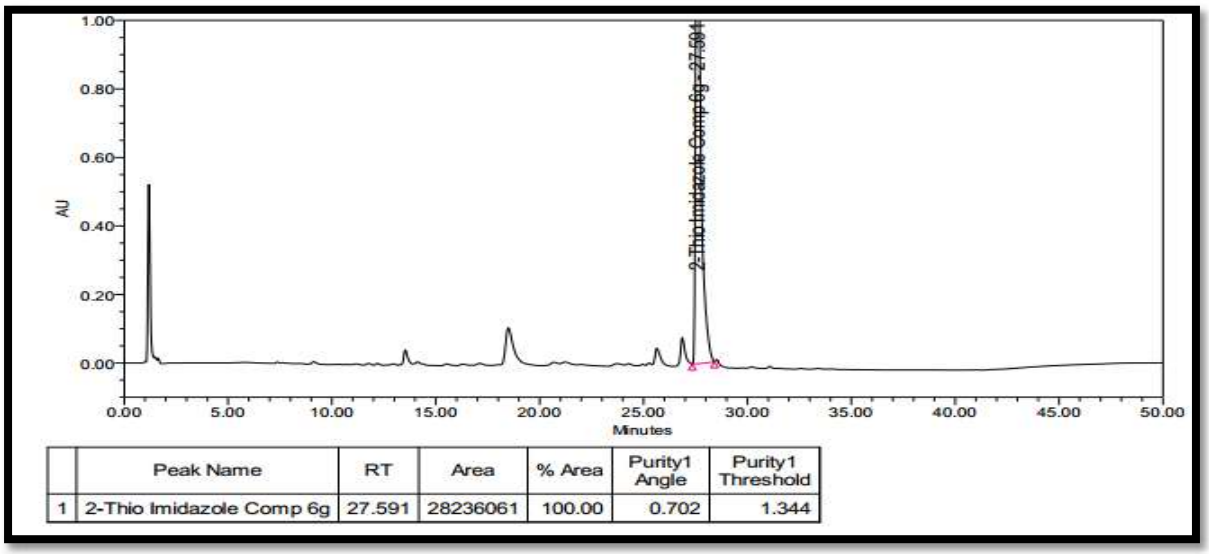

	Peak Name	RT	Area	% Area	Purity1 Angle	Purity1 Threshold
1	2-Thio Imidazole Comp 6g	27.591	28236061	100.00	0.702	1.344

Fig 5.17 Peak purity of oxidation treated sample

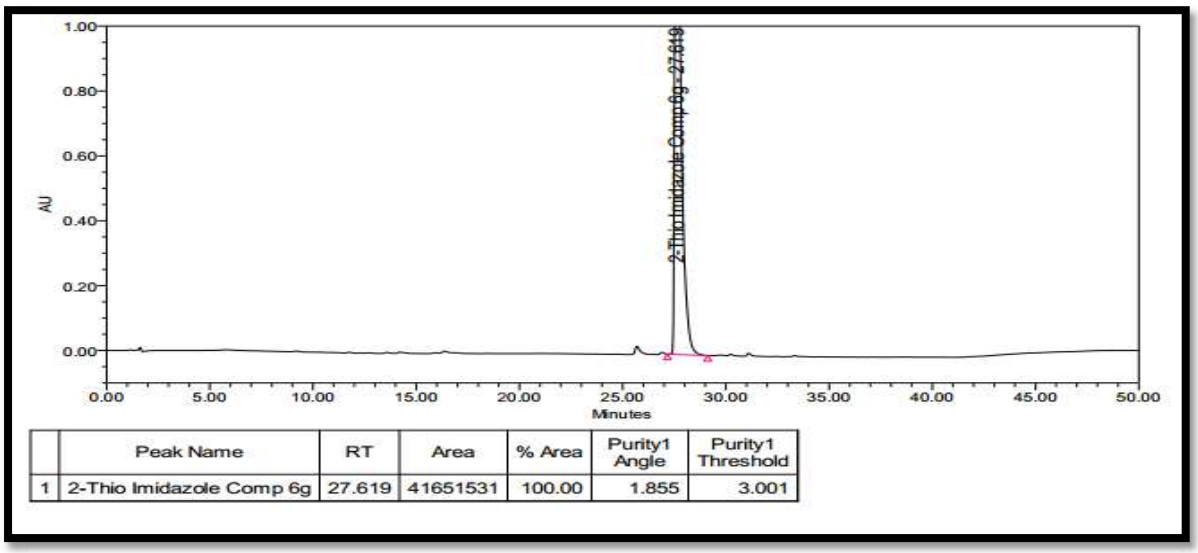

	Peak Name	RT	Area	% Area	Purity1 Angle	Purity1 Threshold
1	2-Thio Imidazole Comp 6g	27.619	41651531	100.00	1.855	3.001

Fig 5.18 Peak purity of UV treated sample

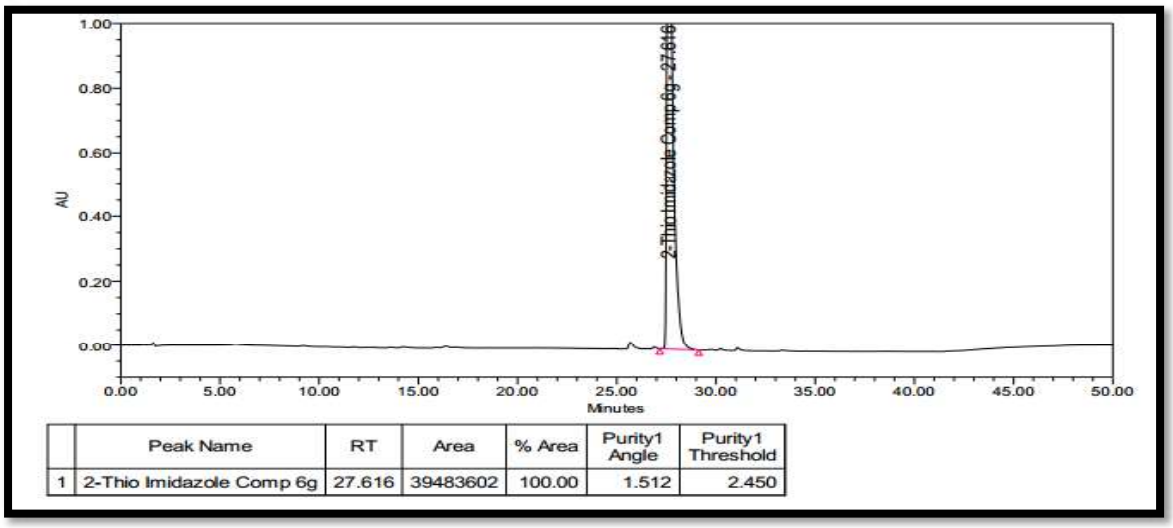

Fig 5.19 Peak purity of thermally treated sample

5.9 Summary of Force Degradation Study

Degradation condition	Time	Temp	Assay (%, w/w)	RS by HPLC %degradation	Mass balance(% assay + % deg. products)	Remarks/observation
A control sample (untreated)	-	-	96.4	2.8	99.2	NA
HCl, 5.0 N (acid degradation)	2 h	60°C	95.0	3.5	98.5	No significant degradation observed
NaOH, 5.0 N (base degradation)	2 h	60°C	93.1	4.1	97.2	No significant degradation observed
Oxidation by 3.0% H2O2	2 h	25°C	79.3	21.02	100.3	Oxidized product was formed
Thermally treated	24 h	105°C	97.1	2.8	99.9	No significant degradation observed
UV treated (254nm)	24 h	25°C	96.9	2.75	99.7	No significant degradation observed

Table 5.13 Summary of degradation study

5.10 Identification of impurity by LC-MS

An electrospray LC-MS system (Shimadzu Prominence HPLC coupled with Triple Quadrupole Mass Spectrometer LCMS-8040 with lab solution software, version 5.72, Japan) was used for identification of degradation impurities formed during stress testing studies. Chromatography was performed on YMC Triat C18 150 mm, 4.6 mm and 3 µm particle size column from YMC co. Ltd. Japan using mobile phase consisting of mobile phase A (10mM ammonium acetate (pH 8.5) with ammonia solution) and mobile phase B (0.1% ammonia in acetonitrile) at a flow rate of 1.2 ml/min. The LC gradient program was applied as per Table 5.10. The column temperature was maintained at 40°C. ACN: water in the ratio of 95:5 %, v/v was used as a diluent. Injection volume was 20µL. The analysis was carried out by using electrospray ionization mode (+ve and -ve). The capillary voltage was at 3500 V and collision energy was -35 V. Desolvation temperature was 250°C with nebulizing gas flow rate 180 L/h. The LC-MS chromatogram is presented in Fig 5.20.

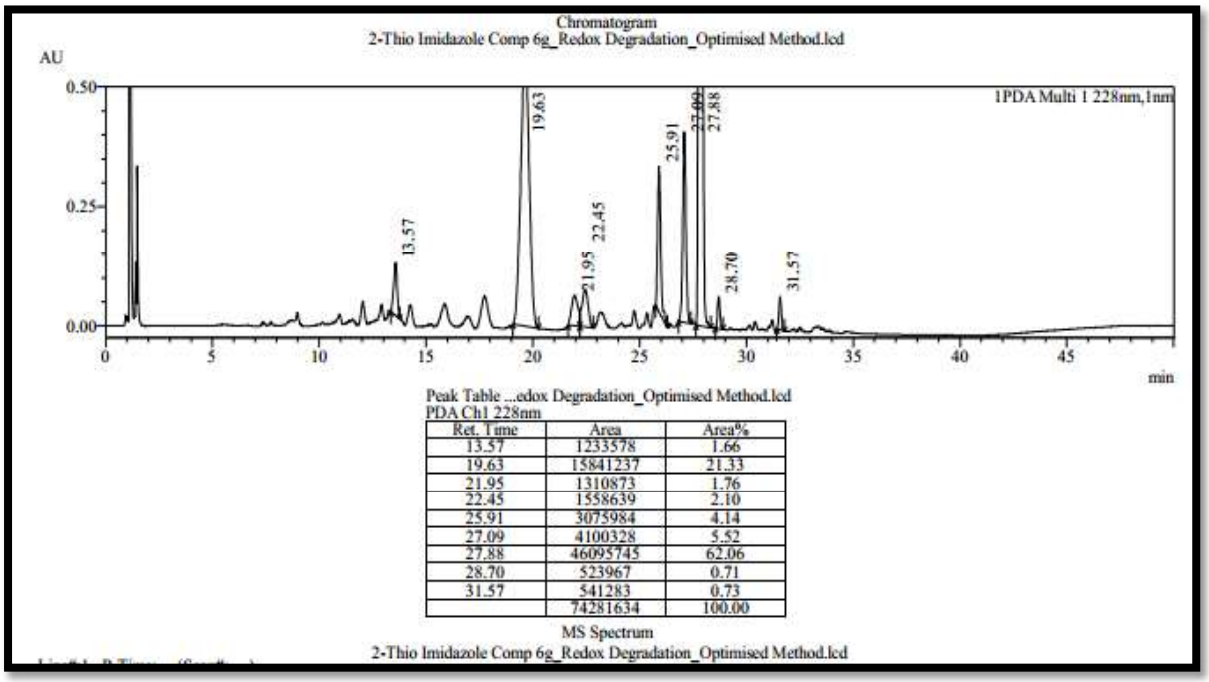

Ret. Time	Area	Area%
13.57	1233578	1.66
19.63	15841237	21.33
21.95	1310873	1.76
22.45	1558639	2.10
25.91	3075984	4.14
27.09	4100328	5.52
27.88	46095745	62.06
28.70	523967	0.71
31.57	541283	0.73
	74281634	100.00

Fig 5.20 LC chromatogram in LC-MS for Oxidative degradation product

Identification of degradation related impurities for the ZY12201 was done in oxidation treated sample through LC-MS technique. One impurity was detected in ZY12201 oxidation treated sample which was confirmed and identified through mass spectral analysis.

The positive ion mass spectral analysis of impurity-1 was observed at 575 (M) suggesting the possibility of Molecular formula $C_{31}H_{31}FN_4O_4S$, which confirms the theoretical molecular weight of Impurity-1.

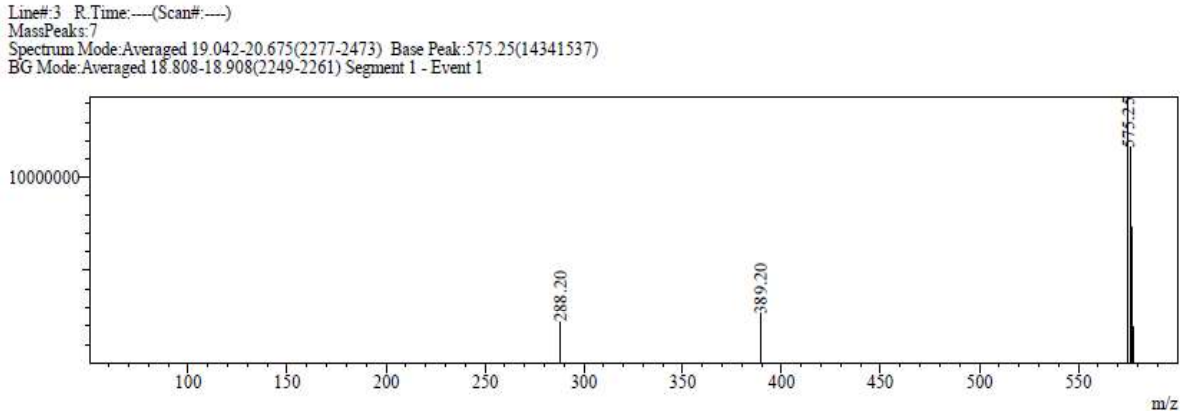

Fig 5.21 Mass spectra of degradation impurity

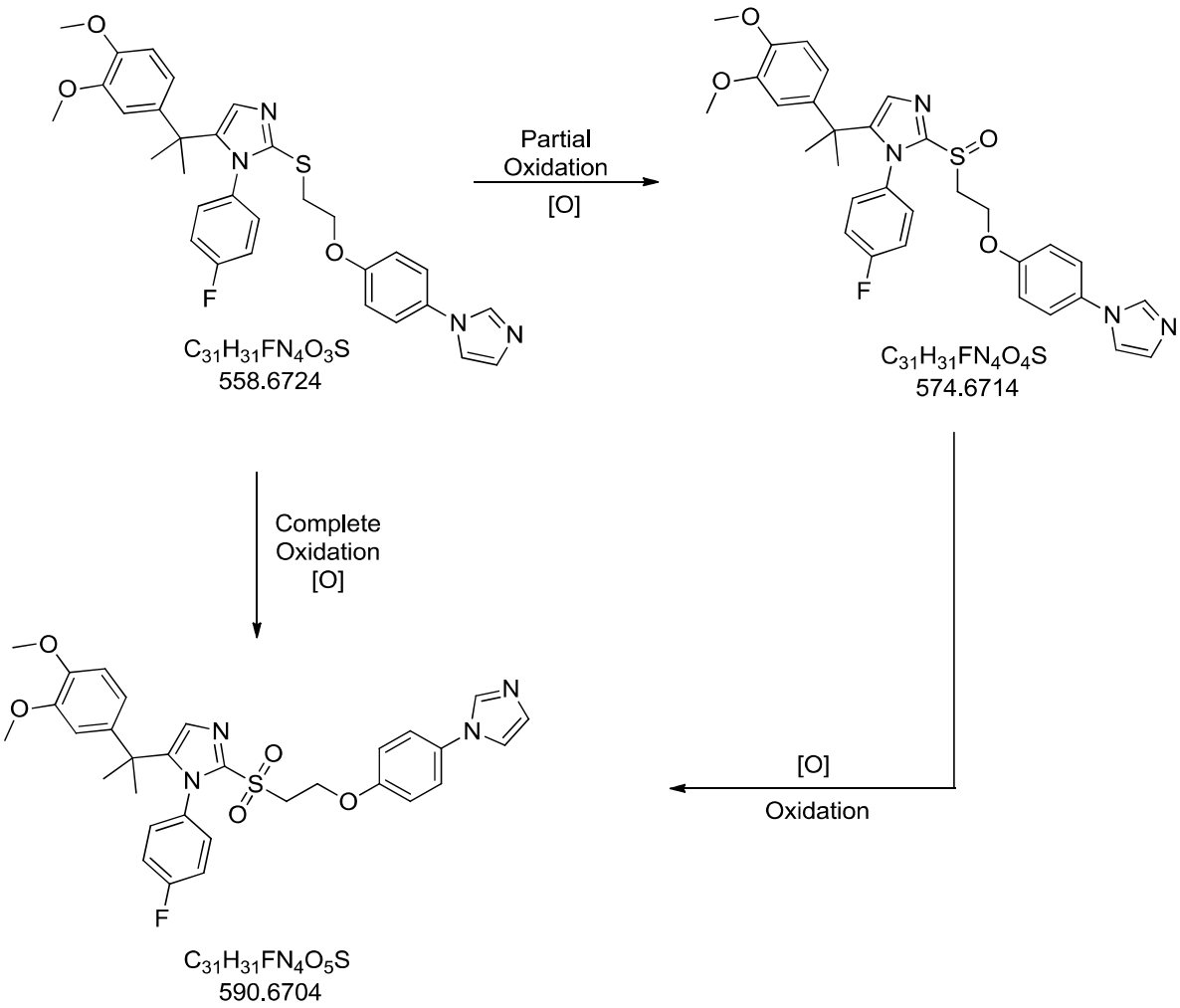

Fig 5.22 Oxidation degradation pathway of ZY12201

5.11 Conclusion:

The analytical method developed in chapter presents a rapid, simple, precise, robust, accurate and selective gradient RP-LC method that separates the ZY12201 and its impurities and degradation products with good resolution. The developed method was validated to ensure the compliance in accordance with ICH guidelines. This method can be used for routine testing and stability analysis in quality control laboratories to checkpurity of ZY12201 in bulk and pharmaceutical formulation.

5.12 References:

1. Rotella CM, Pala L, Mannucci E. Role of insulin in the type 2 diabetes therapy: past, present and future. International journal of endocrinology and metabolism. 2013;11(3):137.
2. Stein SA, Lamos EM, Davis SN. A review of the efficacy and safety of oral antidiabetic drugs. Expert opinion on drug safety. 2013;12(2):153-75.
3. Ashiya M, Smith RE. Non-insulin therapies for type 2 diabetes. Nature Publishing Group; 2007.
4. Sato H, Genet C, Strehle A, Thomas C, Lobstein A, Wagner A, et al. Anti-hyperglycemic activity of a TGR5 agonist isolated from Olea europaea. Biochemical and biophysical research communications. 2007;362(4):793-8.
5. Klindt C, Reich M, Hellweg B, Stindt J, Rahnenführer J, Hengstler J, Köhrer K, Schoonjans K, Häussinger D, Keitel-Anselmino V. The G protein coupled bile acid receptor TGR5 (Gpbar1) modulates endothelin-1 signaling in liver. Zeitschrift für Gastroenterologie. 2020 Jan;58(01):1-.
6. Maruyama T, Miyamoto Y, Nakamura T, Tamai Y, Okada H, Sugiyama E, et al. Identification of membrane-type receptor for bile acids (M-BAR). Biochemical and biophysical research communications. 2002;298(5):714-9.
7. Thomas C, Gioiello A, Noriega L, Strehle A, Oury J, Rizzo G, et al. TGR5-mediated bile acid sensing controls glucose homeostasis. Cell metabolism. 2009;10(3):167-77.
8. Watanabe M, Houten SM, Mataki C, Christoffolete MA, Kim BW, Sato H, et al. Bile acids induce energy expenditure by promoting intracellular thyroid hormone activation. Nature. 2006;439(7075):484.
9. Joshi V, Sojitra C, Sasane S, Shukla M, Chauhana R, Chaubey V, Jain S, Shah K, Mande H, Soman S, Sudhakar P, Shah S, Pandey B, Singh K, Agarwal S. Practical Efficient Synthesis of 2-Thio-imidazole derivative - ZY12201: A Potent TGR5 Agonist. Organic Process Research and Developement. 2020,:
10. Agarwal S, Sasane S, Deshmukh P, Rami B, Bandyopadhyay D, Giri P, Giri S, Jain M, Desai R. Identification of an Orally Efficacious GPR40/FFAR1 Receptor Agonist. ACS Medicinal Chemistry Letters. 2016, 7 (12), 1134–1138:
11. Agarwal S, Patil A, Aware U,Deshmukh P, Darji B, Sasane S, Sairam K, Priyadarsiny P, Giri P, Patel H, Giri S, Jain M, Desai R. Discovery of Novel Orally Bioavailable TGR5 Receptor Agonist. ACS Medicinal Chemistry Letters. 2016, 7 (1), 51–55:

12. Agarwal S, Sasane S, Kumar J, Deshmukh P, Bhayani H, Giri P, Giri S, Soman S, Kulkarni N, Jain M, Evaluation of novel TGR5 agonist in combination with Sitagliptin for possible treatment of type 2 diabetes. Bioorg. Medicinal Chemistry Letter. 2018, 28, 1849-1852.

13. Agarwal S, Sasane S, Kumar J, Darji B, Bhayani H, Soman S, Kulkarni N, Jain M, Novel 2-Mercapto Imidazole and Triazole Derivatives as Potent TGR5 Receptor Agonists. Medicine in Drug Discovery 2019, 1, 100002:

14. Agarwal S, Indian Pat. Appl. (2014), IN 2012MU01499 A 20140110, 10 Jan 2014: Novel compounds and their use for the treatment of metabolic or related disorders.

15. Agarwal S, Jain M, Patel P, PCT Int. Appl. WO 2013/054338, 18 April 2013 (Appl. PCT/IN2012/000471, 4.07.2012): 2-Thio-Imidazole Derivatives as TGR5 Modulators.

16. Agarwal S, Desai R, PCT Int. Appl. WO 2013/102929, 11 July 2013 (Appl. PCT/IN2012/000821, 17.12.2012): Novel Compounds for Treatment of Diabetes, Obesity or related Disorders

17. Agarwal S, Desai R, PCT Int. Appl. WO 2013/164838, 7 November 2013 (Appl. PCT/IN2013/000130, 05.03.2013): Novel Heterocyclic Compounds and their use for treatment of Diabetes, Obesity or related disorders

18. Agarwal S, Aware U, Patil A, Rohera V, Ghate M, Jain M, Patel P, Silica-gel Catalyzed Facile Synthesis of 3,4-Dihydro- pyrimidinones. Bull. Korean Chemistry Society. 2012, 33 (2), 377.

19. ICH DRG, editor. Stability testing of new drug substances and products Q1A (R2). Proceedings of the International Conference on Harmonization, Geneva; 2003.

20. Bajaj S, Singla D, Sakhuja N. Stability testing of pharmaceutical products. Journal of Applied Pharmceutical Science. 2012;2(3):129-38.

21. Guideline IHT, editor. Evaluation for stability data q1e. International Conference on Harmonisation of Technical Requirements for Registration of Pharmaceuticals for Human Use; 2003.

22. Group IEW, editor. Q1A (R2) Stability Testing of New Drug Substances and Products. International Conference on Harmonisation of Technical Requirements for the Registration of Pharmaceuticals for Human Use Geneva: ICH; 2003.

23. Guideline IHT. Impurities in new drug products. Q3B (R2), current step. 2006;4:1-5.

24. Guideline I. Q1B: Photostability Testing of New Drug Substances and Products. ICH Secretariat, Geneva, Switzerland. 1996.

25. Kovaříková P, Klimeš J, Dohnal J, Tisovská L. HPLC study of glimepiride under hydrolytic stress conditions. Journal of pharmaceutical and biomedical analysis. 2004;36(1):205-9.

26. Boccardi G. Oxidative susceptibility testing, pharmaceutical Stress Testing-Predicting Drug Degradation; Baertschi SW, editors. Taylor and Francis, New York; 2005.

27. Alsante KM, Hatajik TD, Lohr LL, Santafianos D, Sharp TR. Solving impurity/degradation problems: case studies. Separation Science and Technology: Elsevier; 2004. p. 361-400.

28. Oyler AR, Segmuller BE, Sun Y, Polshyna A, Dunphy R, Armstrong BL, et al. Forced degradation studies of rapamycin: Identification of autoxidation products. Journal of pharmaceutical and biomedical analysis. 2012;59:194-200.

29. Singh R. Current trends in forced degradation study for pharmaceutical product development. Journal of Pharmaceutical Education & Research. 2012;3(1).

30. Ali NW, Abbas SS, Zaazaa HE-S, Abdelrahman MM, Abdelkawy M. Validated stability indicating methods for determination of nitazoxanide in presence of its degradation products. Journal of pharmaceutical analysis. 2012;2(2):105-16.

31. T kumar T. development and validation of specific stability indicating analytical methods for some active pharmaceutical ingredients. Bharathidasan University, 2012.

32. Annapurna MM, Mohapatro C, Narendra A. Stability-indicating liquid chromatographic method for the determination of Letrozole in pharmaceutical formulations. Journal of pharmaceutical analysis. 2012;2(4):298-305.

33. Kats M. Forced degradation studies: regulatory considerations and implementation. 2005.

34. Alsante KM, Ando A, Brown R, Ensing J, Hatajik TD, Kong W, et al. The role of degradant profiling in active pharmaceutical ingredients and drug products. Advanced drug delivery reviews. 2007;59(1):29-37.

35. Gupta A, Yadav JS, Rawat S, Gandhi M. Method development and hydrolytic degradation study of Doxofylline by RP HPLC and LC–MS/MS. Asian J Pharm Anal. 2011;1:14-8.

36. Allwood M, Plane J. The wavelength-dependent degradation of vitamin A exposed to ultraviolet radiation. International journal of pharmaceutics. 1986;31(1-2):1-7.